

Rodent paleofaunas as indicators of climatic change in Europe during the last 125,000 years

Manuel Hernández Fernández*

Departamento de Paleobiología, Museo Nacional de Ciencias Naturales (CSIC), José Gutiérrez Abascal, 2, 28006 Madrid, Spain

Departamento de Paleontología, Facultad de Ciencias Geológicas, Universidad Complutense de Madrid, Ciudad Universitaria, 28040 Madrid, Spain

Received 12 October 2004

Available online 30 January 2006

Abstract

This paper presents a quantitative reconstruction of the European late Pleistocene paleoclimate based on 72 rodent assemblages of five sequences from France, Germany and Bulgaria, covering the last interglacial–glacial cycle. They show a pattern of severe changes in temperature, with reduced precipitation during the coldest periods. A tentative correlation between the isotopic and palynological records and the paleotemperature changes is shown. These changes are consistent with variations in atmospheric circulation patterns in response to an expanding–retracting Fennoscandian ice-sheet. They can be attributed to the enhancement–weakening of the Scandinavian-Polar anticyclone and its associated dry winds, the south–north shifting of the North Atlantic Polar Front, and the varying supply of moist air from the Atlantic. Qualitative paleoenvironmental analysis shows broadleaved-deciduous forests in France and Bulgaria during most of the studied period. Taiga and tundra appeared in eastern France during the lower Würm. The German sequence indicates the presence of coniferous forests. These results are broadly consistent with other paleobiological records (mammalian, avian and insect faunas, isotopic record in dental tissue, palynology). The main discrepancies with the paleoclimate inferred from the palynological record are found during the coldest periods and are probably due to the interaction between vegetation, climate, and atmospheric CO₂ levels.

© 2005 University of Washington. All rights reserved.

Keywords: Atmospheric CO₂; Bioclimatic analysis; Global atmospheric circulation; Mammalia; Paleoclimatology; Paleoecology; Pleistocene; Quaternary; Rodentia; Weichselian Glaciation

Introduction

The understanding of past climate and the mechanisms of climate change remain major challenges in science. Geological evidence indicates that at several points on the history of Earth, climates have fluctuated between glacial and interglacial stages. Although the study of Pleistocene climates began more than a century ago, it is only in the 1970s that the synthesis of the previous studies and the new oceanographic data allowed the reconstruction of the Earth climate during the last glacial maximum (CLIMAP, 1976). Afterwards, the studied time lapse was extended to the Holocene and the climate of the last 18,000 yr was reconstructed in 3000-yr intervals (COHMAP, 1988). Recently, the project BIOME 6000 (Prentice and Webb, 1998;

Prentice et al., 2000) has developed global paleovegetation databases that allow the reconstruction of the global distribution of biomes for the last glacial maximum and the middle Holocene. Today, the improvement of the time resolution in the paleoceanographic studies and the increase in number of terrestrial sequences is starting to allow the temporal extension of high-resolution paleoclimatic studies backwards into the late Pleistocene, including the last interglacial–glacial cycle (Kershaw and Whitlock, 2000; van Andel, 2002; Barron and Pollard, 2002; Cosgrove et al., 2002; Huntley et al., 2003).

Guiot et al. (1989) argued that palynological analysis generates the most reliable climatic data in the continental record. Nevertheless, the climate–vegetation interrelationship is influenced by the CO₂ concentration in the atmosphere, which may produce incorrect paleoclimatic reconstructions (Betts et al., 1997; Farquhar, 1997; Cowling, 1999; Cowling and Sykes, 1999). On the other hand, the existence of vegetation patterns with no current analogues (Overpeck et

* Departamento de Paleobiología, Museo Nacional de Ciencias Naturales (CSIC), José Gutiérrez Abascal, 2, 28006 Madrid, Spain.

E-mail addresses: mhernandez@mncn.csic.es, hdezfdz@geo.ucm.es.

al., 1992) has given rise to the development of new paleoclimatic methodologies that combine palynology with data from other fields (Guiot et al., 1993). I present here an independent paleoclimatic analysis of the last interglacial–glacial cycle on Europe, which is based in rodent faunas. They are considered a suitable climatic indicator for climatic reconstructions (see references in Hernández Fernández, 2001) and may complement the paleoclimatic reconstructions produced by other lines of evidence.

Materials and methods

Faunal assemblages

I have compiled from the literature faunal lists from five sequences of rodent-bearing fossil sites in Europe (Fig. 1). They are La Chênélaz (eastern France; Jeannet and Cartonnet, 2000; Schweizer, 2002), Gigny (eastern France; Campy et al., 1989; Chaline et al., 1995), Kemathenhöhle (southern Germany; von Koenigswald, 1978), Karlukovo (northeastern Bulgaria, Popov et al., 1994) and Bacho Kiro (central Bulgaria; Kowalski and Nadachowski, 1982; Nadachowski, 1984, 1991; Brunet-Lecomte et al., 1992). This study concentrates on these five localities because it is from there where the most comprehensive studies of small mammal assemblages from the late Pleistocene have been undertaken. Nevertheless, the climatic implications inferred below have regional significance, certainly for central Europe and probably for much of the continent. Since an exhaustive sampling of the assemblages is essential to avoid some methodological problems, only faunas with more than 100 rodent molars (M1 + M2 + m1 + m2) have been included in the analysis. Faunas with fewer teeth are considered not to be representative enough (van de Weerd and Daams, 1978; Daams et al., 1999). Dating for different levels of these sequences is available (Table 1). Additionally the level Gigny XXI has been dated between 211,000 and 100,000 yr ago,

Table 1

Radiocarbon (^{14}C) dates associated to the studied rodent assemblages

Assemblage	Radiocarbon age		References
	^{14}C yr B.P.	$\pm\sigma^a$	
La Chênélaz 1	1000	n.a	Jeannet and Cartonnet, 2000
La Chênélaz 2a	2440	n.a	Jeannet and Cartonnet, 2000
Karlukovo 16 I	7000	1,000	Popov et al., 1994
La Chênélaz 2b	9530	n.a	Jeannet and Cartonnet, 2000
La Chênélaz 2c	12,610	n.a	Jeannet and Cartonnet, 2000
Kemathenhöhle b'	24,400	326	von Koenigswald, 1978
Gigny V	24,430	500	Campy et al., 1989
La Chênélaz 5b	25,670	n.a	Jeannet and Cartonnet, 2000
Bacho Kiro 6a/7	29,150	950	Kowalski and Nadachowski, 1982
Kemathenhöhle b1 Low	30,910	660	von Koenigswald, 1978
Karlukovo 16 VI	31,000	1,750	Popov et al., 1994
Gigny IX	>31,500	n.a	Chaline et al., 1995
Gigny XI	>33,000	n.a	Chaline et al., 1995
La Chênélaz 6b	33,380	n.a	Jeannet and Cartonnet, 2000; Schweizer, 2002
Kemathenhöhle b2	33,380	933	von Koenigswald, 1978
Kemathenhöhle e	43,900	3,880	von Koenigswald, 1978
Bacho Kiro 11	52,500	6,500	Kowalski and Nadachowski, 1982
Bacho Kiro 13	>47,000	n.a	Kowalski and Nadachowski, 1982

^a n.a., not available.

using the ESR and $^{230}\text{Th}/^{234}\text{U}$ methods. This suggests that the studied assemblages cover the period between the marine oxygen isotope stages (OIS) 1 and 5–6. Overall, the study presented here includes data derived from 72 rodent assemblages, which date from 1000 to ca. 125,000 yr ago.

Bioclimatic analysis

In this study, qualitative and quantitative models developed for the bioclimatic analysis of rodent faunas are used. Hernández Fernández (2001) and Hernández Fernández and Peláez-Campomanes (2003, 2005) give a step-by-step account of the method as it was used in those studies. Below the method is explained in a more general way.

The models are based on 454 extant rodent species from fifty localities all over the world, resulting in a database with 861 presence records of these species in the studied localities. The fifty studied localities, from which there is available information on both fauna and climate, were selected in a way that they cover all the climate zones (according to Walter, 1970), they are as widely scattered as possible, and they represent the average climatic conditions within their corresponding climate zone. The sampling area of each locality is 10,000 km², which is adequate to take into consideration all possible regional habitats. In order to have comparable data for all the biomes, the database contains five localities from each of the ten considered biomes. Information on these fifty localities and references used to obtain the faunal lists can be consulted in Hernández Fernández (2001).

Because of its simple nomenclature and coincidence with traditional biomes, the climatic typology of Walter (1970) was selected for the bioclimatic characterization of the rodent

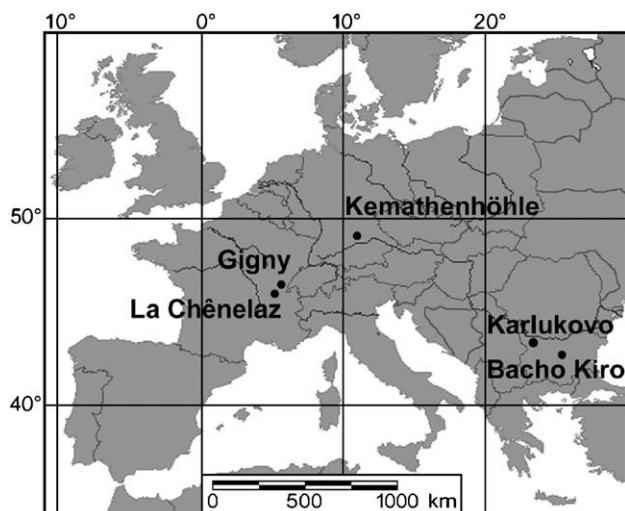


Figure 1. Location of the five Quaternary sequences of rodent paleofaunas used in this work.

faunas. For every locality a species-by-climate matrix is made. The value assigned to each of the species in each climate is 0 when the species does not live in that climate zone or $1/n$ (called the Climatic Restriction Index, CRI; Hernández Fernández, 2001) when it does live on it, n being the number of climates in which the species is present. See Hernández Fernández (2001) for a detailed description of the determination of the climate zones inhabited by a species.

Most of the species recorded in the fossil assemblages are still living in Eurasia. Nevertheless, four species have gone extinct since the last glacial maximum. The bioclimatic characterization of *Spermophilus superciliosus*, *Microtus grafi* and *Dicrostonyx gulielmi* has been carried out by analogy with their closest modern relatives, respectively, *S. major*, *M. multiplex* and *M. subterraneus* and *D. torquatus* (Chaline, 1972; Brunet-Lecomte et al., 1992; Nord Andreassen, 1997). The closest relatives of *Allocricetus bursae* are found in the modern genera *Phodopus*, *Allocricetulus* and *Cricetus* (Koby and Spahni, 1956; Hír, 1993a,b; Kálin, 1999). One problem of the bioclimatic analysis may be that the climatic tolerances of a fossil taxon may be different from those of its nearest living ecological analogue. Nevertheless, influence of this kind of error is weak because the whole rodent fauna from an assemblage is used for the climatic inference of the locality (Hernández Fernández and Peláez-Campomanes, 2003).

Another term introduced by Hernández Fernández (2001) is the Bioclimatic Component (BC), which is the representation in a specific locality of each of the ten existing climates. Ten BC values for each locality are calculated according to the formula:

$$BC_i = (\sum CRI_i)100/S$$

in which i is climate zone i , and S is the number of species in the locality. Each BC value may be understood as the percentage of the faunal assemblage that is characteristic of the corresponding climate. The ten BC values of a locality constitute its bioclimatic spectrum. The use of bioclimatic components (BCs) helps to solve the problem of classifying paleoecological records by reducing the number of entities considered (only 10 BCs) and by providing an ecological basis for treating mammals from different regions in a compatible way.

Hernández Fernández and Peláez-Campomanes (2003) developed explicit algorithms to assign mammal faunas to biomes after the bioclimatic spectra of all the localities were calculated. The quality of these algorithms was evaluated by the proportion of correct assignments of modern faunas to the biomes in which they live. The qualitative bioclimatic model for rodent faunas generated correct climatic classifications for 94% of the studied localities. Subsequently, Hernández Fernández and Peláez-Campomanes (2005) developed transfer functions, based on multiple linear regression, that produce quantitative values for as many as eleven climatic factors as a function of the bioclimatic spectrum (Table 2). Performance of these transfer functions is generally comparable to those based on other proxy indicators such as pollen or insects (Table 2). In order to validate both qualitative and quantitative

Table 2

Climatic variables inferred by the quantitative bioclimatic analysis of rodent faunas and statistics for each multiple regression model

Abbreviation	Climatic factor	Units	r^2	SE
T	Annual mean temperature	°C	0.930	3.637
T_p	Annual positive temperature	0.1°C	0.911	362.682
T_{max}	Mean temperature of the warmest month	°C	0.746	4.754
T_{min}	Mean temperature of the coldest month	°C	0.932	5.081
M_{ta}	Mean annual thermal amplitude	°C	0.779	6.408
I_t	Thermicity index	0.1°C	0.938	130.569
I_c	Compensated thermicity Index	0.1°C	0.948	94.587
VAP	Vegetative activity period	months	0.955	0.949
FVAP	Free vegetative activity period	months	0.918	1.337
P	Annual total precipitation	mm	0.746	470.615
D	Drought length	months	0.926	1.306

Note. For an explanation of each variable see Hernández Fernández and Peláez-Campomanes (2005). r^2 , determination coefficient; SE, standard error of the estimate.

bioclimatic models, new localities were studied by Hernández Fernández and Peláez-Campomanes (2003, 2005), providing additional information for a total of 1080 locality records of 500 rodent species. The results of these validations were highly satisfactory.

Since climate change evokes differential responses in the taxa constituent of ecological communities (FAUNMAP, 1996), bioclimatic analysis must deal with the occurrence of non-analogous faunas. Nevertheless, the bioclimatic spectrum is an emergent property of the community based on functional bioclimatic characteristics of its constituent taxa (Hernández Fernández and Peláez-Campomanes, 2003), which makes the bioclimatic analysis fairly independent of modern analogue communities. Another potential limitation in this methodology is the existence of past unknown biomes. However, the models for quantitative paleoclimatic inference address this problem because, as an extrapolating method, the transfer functions can generate paleoclimatic values from all given mammalian components, even when the paleocommunities had no modern analogues. Anyhow, Plio-Pleistocene biomes were largely equivalent to modern ones (CLIMAP, 1976; PRISM, 1995).

Results and discussion

The bioclimatic spectra obtained for the studied fossil rodent associations are shown in Appendix A.

Quantitative bioclimatic analysis

Appendix B shows the values for the different climatic variables in each rodent assemblage as determined by the quantitative bioclimatic models. Figure 2 is based on these data and shows the evolution of mean annual temperature in Europe during the last interglacial–glacial cycle. It includes the isotope ^{18}O curve for the last 123,000 yr, derived from the North Greenland Ice Core Project (NGICP, 2004), and the percentage of arboreal pollen in the palynological record from

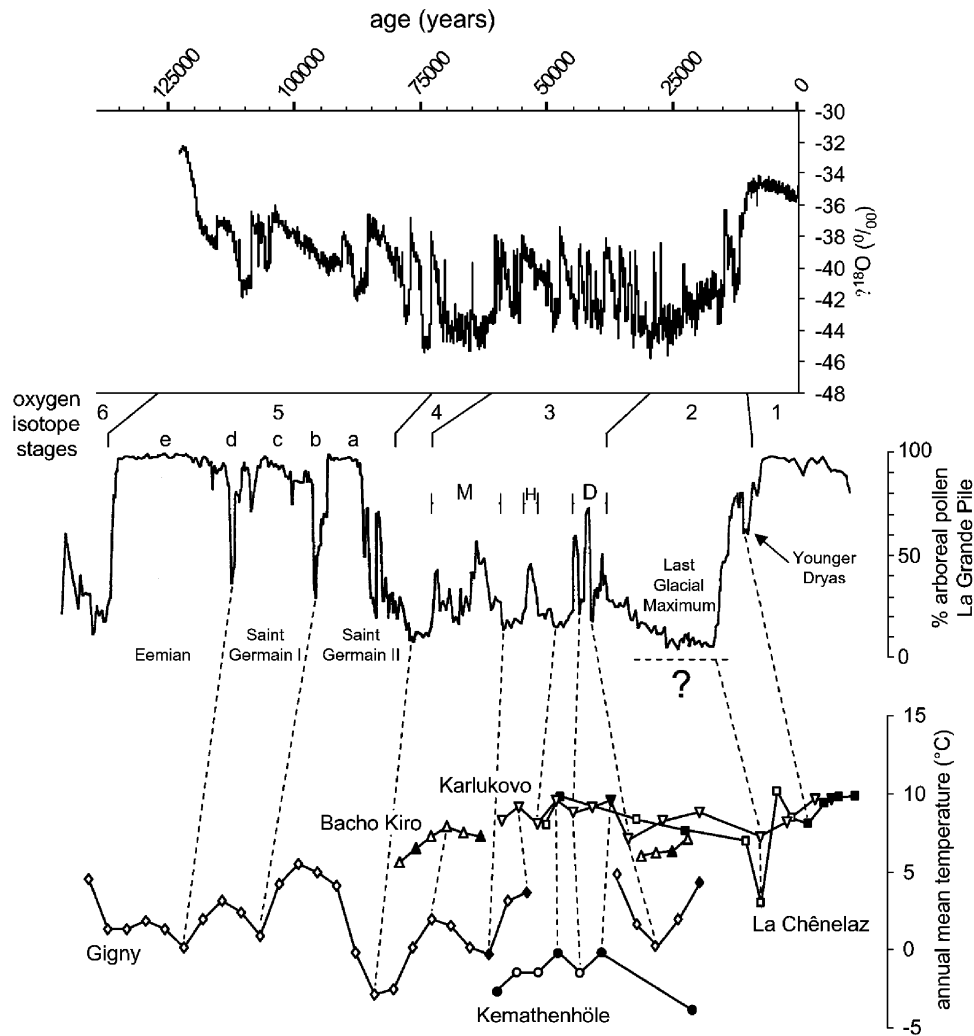


Figure 2. Tentative correlations among the paleotemperature curves of the fossil assemblages studied here, the curve of arboreal pollen from La Grande Pile (Woillard and Mook, 1982) and the isotopic curve of the North Greenland Ice Core Project (NGICP, 2004). Levels in the rodent sequences were plotted roughly uniformly. Discontinuities within the Bacho Kiro and Gigny sequences are due to the presence of levels with small samples of rodent faunas. Black symbols correspond to dated levels (see Table 1). M, Moershoofd interstadial complex; H, Hengelo interstadial; D, Denekamp interstadial.

La Grande Pile, about 150 km to the Northeast of Gigny (Woillard, 1979; Woillard and Mook, 1982). There are perceptible relationships among these three records. Gigny and Bacho Kiro sequences show potential hiatuses due to the presence of levels with a small sample size in their rodent assemblages ($M1 + M2 + m1 + m2 < 100$; Daams et al., 1999). Gigny sequence probably covers the final part of the Eemian (OIS 5e), the Pre-Würmian (OIS 5d-a), Eowürmian or lower Würmian (OIS 4), and the middle Würmian (OIS 3). According to the dating of the most recent level in Gigny (Gigny V, 22,430 ^{14}C yr B.P., Chaline et al., 1995), only the beginning of the Würmian pleniglacial (OIS 2) is recorded. Climatic events related to the last glacial stage (OIS 2) and the Younger Dryas, however, have been recorded in the sequences from La Chênélaz and Karlukovo. Nevertheless, the relatively high temperature in the coldest moment of these sequences indicates that the last glacial maximum was not recorded. The few radiometric dates in the Gigny sequence and the presence of sampling and sedimentary hiatuses (Campy et al., 1989; Chaline et al., 1995) make it difficult

to establish a tight correlation between the paleotemperature curve obtained and the isotopic record. Nevertheless, the former has certain characteristics that make a tentative correlation between the curves possible at several points (Fig. 2). The initial phase of the sequence has palynological characteristics that reflect the transition from a warm climate to a temperate one (Chaline et al., 1995), which is typical of the Eemian. Although it disagrees with Chaline et al. (1995), who argue that there is a hiatus during the OIS 5d-4, it seems apparent that the coldest point correlates to the OIS 4. This agrees with the results of Navarro et al. (2004), based on the isotopic composition of rodent teeth from the Gigny sequence. Before this point, there are two relative temperature maximums, which might be correlated with the interstades Saint Germain I (OIS 5c) and Saint Germain II (OIS 5a). Nevertheless, Navarro et al. (2004) have correlated this part of the sequence with interstades within OIS 4. Since there is not a high-resolution chronology associated to this part of the sequence, the correlation with the global isotopic record remains tentative. Several temperature peaks are observed

during the OIS 3, which might be correlated with different interstades described in the Netherlands and detected in the pollen record of La Grande Pile (Woillard and Mook, 1982) or the isotopic record from paleoceanographic cores (Dansgaard et al., 1993). They are the Moershoofd interstadial complex and the Hengelo and Denekamp interstades. Based on ^{14}C dates, the paleotemperature maximums at Kemathenhöhle correlate with some of the thermal maximums detected in the middle Würm, possibly during the Denekamp interstade. The first part of the Karlukovo sequence appears to correlate with the Hengelo and Denekamp interstades, but there is only one radiometric date associated to this part of the sequence. The oldest part of Bacho Kiro sequence dates to the Moershoofd interstadial complex, while its younger part represents a phase of temperature increase during the Denekamp interstade.

Annual positive temperature (T_p), mean temperature of the coldest month (T_{\min}), mean temperature of the warmest month (T_{\max}), thermicity index (I_t), compensated thermicity index (I_{tc}) and vegetative activity periods (VAP and FVAP) are positively correlated and, therefore, behave in a similar way to the mean annual temperature (not shown). Consequently, they will not be further discussed here. There is also a highly significant correlation between the decrease in temperature and the increase in continentality, here expressed as the temperature range between T_{\max} and T_{\min} (Fig. 3), i.e., during the glacial periods there was a significant increase in continentality in the European climate.

Figure 4 shows that in general, temperature increases coincide with an increase in precipitation, which oscillates between 600 and 1000 mm in Gigny, while in La Chênélaz fluctuates between 1000 and 1600 mm. Bacho Kiro and Karlukovo occupy an intermediate position (800–1400 mm), while Kemathenhöhle presents the lowest rainfall pattern of the four sequences (500–700 mm). It is interesting to note that central Bulgaria today receives lower precipitations than eastern France or southern Germany.

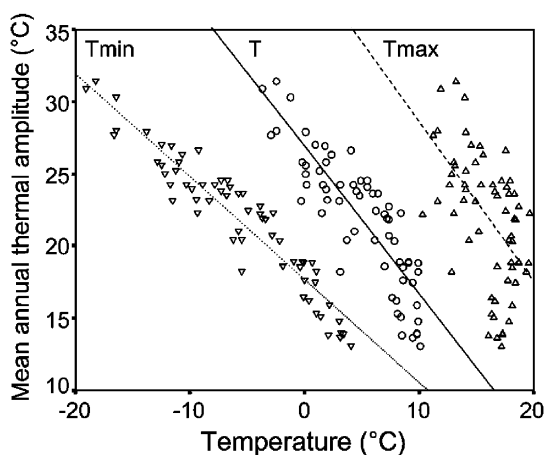


Figure 3. Relationship between mean annual thermal amplitude and mean temperature of the coldest month (T_{\min} ; inverse triangles, dotted line; $r^2 = 0.912$, $P < 0.001$), mean annual temperature (T ; circles, solid line; $r^2 = 0.766$, $P < 0.001$), and mean temperature of the warmest month (T_{\max} ; triangles, dashed line; $r^2 = 0.307$, $P < 0.001$) during the last interglacial–glacial cycle in Europe.

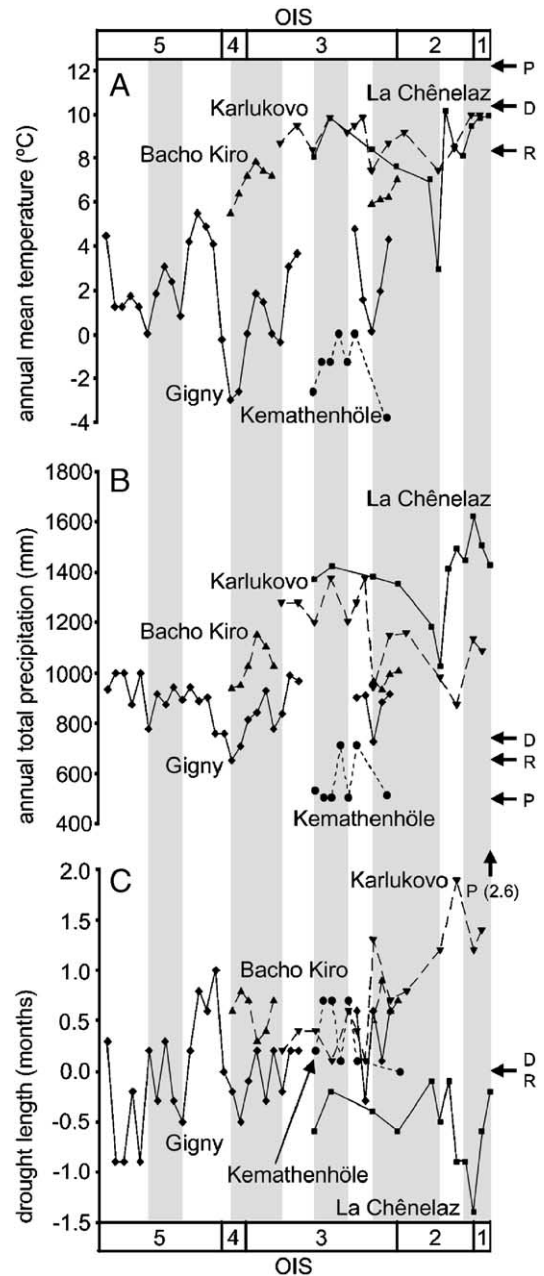


Figure 4. Evolution of the mean annual temperature, annual total precipitation and drought length in La Chênélaz (squares), Gigny (diamonds), Kemathenhöhle (circles), Bacho Kiro (triangles), and Karlukovo (inverse triangles). The relative temporal placement of the five sequences is approximate and derived from Figure 2. The marine oxygen isotope stages (OIS) are shown. Grey and white bars correspond to different interstadial stages as shown in Figure 2. Arrows on the right point out the current climatic values in close localities (Arléry, 1970; Meteorological Office, 1972): D, Dijon (eastern France); R, Regensburg (southern Germany); P, Plovdiv (central Bulgaria).

Drought length is never severe (≤ 2 months). Although during part of the studied period it has values lower than 0, which is a mathematical artifact, it shows a comprehensible pattern (Fig. 4). During the increasingly warm Postglacial, drought length drops to the lowest levels of the sequence in La Chênélaz, and to the highest ones in Karlukovo. Nevertheless, during the Würmian Glaciation, aridity peaks in Gigny and Kemathenhöhle coincide with the interstades.

This may be related to the increase in potential evapotranspiration (PET) that is associated with the increase in temperature. In Bacho Kiro, however, there is an “intermediate” pattern in which the most arid intervals occur during the transitional phases between cool and warm phases, not in the temperature relative maximums. This might be due to its southern geographical position and its consequently higher temperatures than in the other sequences. During the warmest intervals of the Würmian glaciation, Bulgaria presents warm conditions (with high precipitations and, therefore, low drought length). During the coldest periods, the low temperatures and the consequent decrease of PET imply also low levels of aridity. Only in the intermediate climatic stage there is an increase in drought length because the temperatures are high enough to produce a significant drought period. This intermediate pattern is also seen in the initial part of the sequence from La Chênélaz, where temperatures are similar to those in Bacho Kiro, and in most of the Karlukovo sequence. Nevertheless, this sequence shows that at the end of the Pleniglacial there is a significant increase in drought length, which suggests a profound change in the regional climate of southeastern Europe during this time.

Figure 5 shows that, in general, drought length increases with temperature but when certain temperature threshold (which could be defined as the limit between cold and warm climatic regimes) is surpassed there is decrease in aridity. This is true for both the mean annual temperature (not shown) and the mean temperature of the coldest month, although the quadratic regression is not significant (Fig. 5). Nevertheless, with the mean temperature of the warmest month (Fig. 5), the reverse pattern is observed, because during the intermediate climatic stage the higher continentality implies that the summer temperatures are higher than during the warm phase.

Summarizing, during intervals with intermediate temperatures in the Würmian Glaciation, there is an increase of aridity, which attains the maximum values of the studied period. This is despite the increase in precipitation, probably because there is an increase in PET associated with increased temperature. This suggests an intensification of the hydric seasonality during these times. Guiot (1990) and Prentice et al. (1992) have

reported an increase in seasonality in the Mediterranean areas during the glacial periods.

All these changes are related to the alteration of the atmospheric global circulation provoked by the formation of huge ice sheets over the northern continents during the glacial periods (Fig. 6). Large and permanent anticyclonic circulation developed over the Fennoscandian ice sheet, generating surface continental winds coming from the East, which were responsible for the decrease in precipitation (Broccoli and Manabe, 1987; COHMAP, 1988; Woodcock and Wells, 1990; Harrison et al., 1992). Additionally, during the glacial periods, the Westerly Jet Stream associated with the precipitation-bearing middle-latitude cyclones of the Polar Front circulated faster (Leroux, 1993) and was displaced to the south (COHMAP, 1988; Meyer and Kottmeier, 1989; Spaulding, 1991; Florineth and Schluchter, 2000). As a result of these processes, the European full-glacial climate was characterized by enhanced frequency of cyclonic storms in the southern areas of Europe, generating an increase in precipitation in the Mediterranean regions, which are arid during the interglacial periods (Spaulding, 1991; Florineth and Schluchter, 2000). However, in central and western Europe, the rainfall diminished because the anticyclone over the Fennoscandian ice sheet, the reduced water carrying capacity of the surface western winds over the cold Atlantic Ocean, and the southern displacement of the Polar Front provoked a strong trend towards the reduction in precipitation over this area (Broccoli and Manabe, 1987; Prentice et al., 1992; Florineth and Schluchter, 2000). Therefore, we see a cold climatic regime in central and western Europe, while Bulgaria is under the conditions of a intermediate climatic regime with moderate aridity (Fig. 6).

During the transitional glacial–interglacial phase, the polar ice-sheet and the associated dry eastern surface winds start retreating (Fig. 6). The southern areas are no longer under their influence, being transferred to a warm-humid climatic regime. The intermediate climatic regime is installed over central and western Europe.

During the interglacial phase, the polar ice sheets are significantly reduced, the influence of the polar winds is restricted to the high latitudes (Strahler and Strahler, 1987), and thus there is an increase in precipitation and a decrease of aridity in central and western Europe. Additionally, the

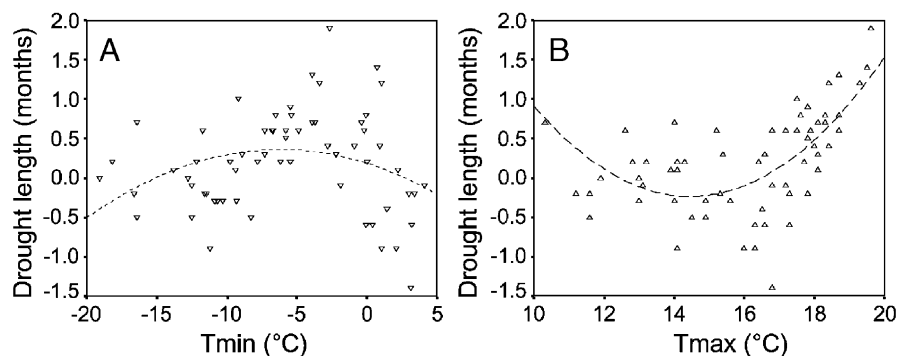


Figure 5. Relationship between drought length and (A) mean temperature of the coldest month (T_{min} ; inverse triangles), or (B) mean temperature of the warmest month (T_{max} ; triangles) during the last European interglacial–glacial cycle. The quadratic regression curves are shown: dotted line, T_{min} , ($r^2 = 0.077$, $P = 0.063$); dashed line, T_{max} , ($r^2 = 0.393$, $P < 0.001$).

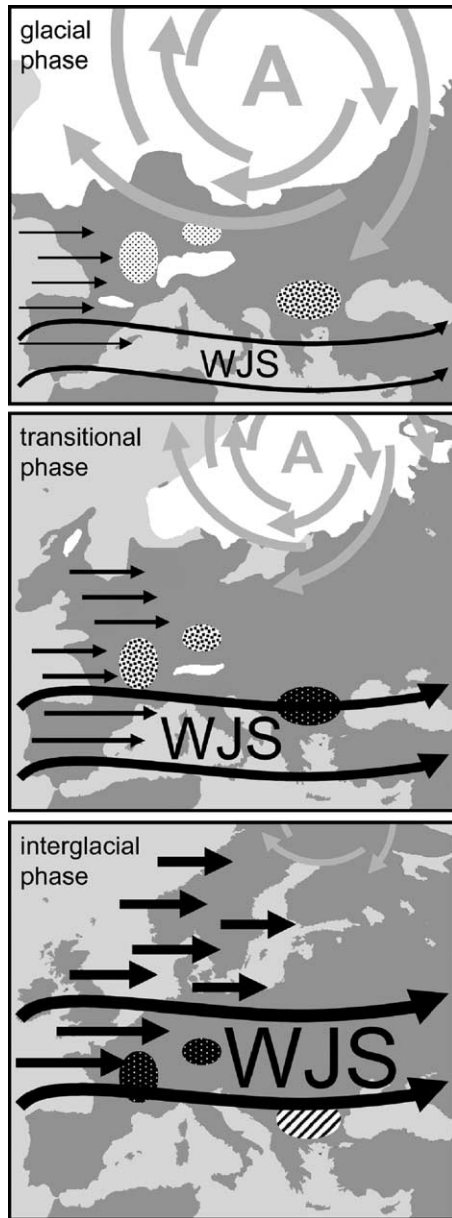


Figure 6. Proposed scenario for the changes in the European climate during the transition between glacial and interglacial stages. The evolution of the climatic regimes in the studied areas is shown: cold regime, light dotted areas; intermediate regime, heavy dotted areas; warm-humid regime, black areas; warm-dry regime, striped areas. WJS, approximate path of the Westerly Jet Stream. A, Scandinavian-Polar anticyclone. Arrows indicate main winds: grey, dry winds; black, humid winds. The thickness and length of the black arrows is proportional to their strength and water carrying capacity. Ice sheets and shoreline reconstructed after COHMAP (1988), Lundqvist and Saarnisto (1995), Ray and Adams (2001), Barron and Pollard (2002) and Svendsen et al. (2004).

Westerly Jet Stream is moved farther north and the surface western winds have a higher water carrying capacity (Fig. 6). Thus, the northern areas benefit from a warm-humid climatic regime. An additional warm-dry climatic regime develops in the Mediterranean area, which have a marginal effect on Bulgaria (2.6 months of drought today). The sudden transition from warm-humid to warm-dry regime observed in Karlukovo during the final part of the Pleniglacial and the Postglacial

supports the influence of the Westerly Jet Stream on the climatic patterns observed.

Qualitative bioclimatic analysis

Table 3 shows the results of the qualitative bioclimatic analysis. They indicate that most of the assemblages in France and Bulgaria have been assigned to the typical temperate climate zone (nemoral broadleaf-deciduous forest biome, VI). The boreal climate zone (taiga biome, VIII) has been found only in two assemblages of Gigny (Gigny XV1 and Gigny XV bottom). The arctic climatic zone (tundra biome, IX) is only found in Gigny XV2, which was above correlated with the Eowürmian (OIS 4). The taiga biome was probably largely distributed in southern Germany because all the levels of Kemathenhöhle have been classified in the boreal climate zone.

Table 3 also shows the climatic assignments that can be made as a function of the climatic data inferred for each fossil site by means of the quantitative bioclimatic models. These climatic assignments have been made using the climatic values inferred for each fossil rodent fauna (Appendix 2) and the keys provided by Allué Andrade (1990) and Walter (1970), Strahler and Strahler (1987), and Rivas Martínez (1994) to designate the climate of each assemblage according to, respectively, Walter's (1970), Köppen's (1931) and Rivas Martínez's (1994) climatic classifications.

Though in most cases the quantitative and the qualitative approaches are consistent, during the Prewürmian and Würmian of Gigny, there are several discrepancies between the climate determined by the qualitative analysis and the one determined quantitatively. For example, while Gigny XII has been classified in the biome VI (nemoral forest) by the qualitative analysis, the quantitative analysis generates climatic values that are circumscribed within the biome VIII (taiga).

A potential cause of this apparent inconsistency might be that the birch (*Betula* sp.) was very important in the main vegetal formations during this period, as deduced from the pollen diagrams from La Grande Pile, about 150 km to the northeast of Gigny (Woillard, 1979) and Les Echets, about 100 km to the southwest (de Beaulieu and Reille, 1984). This is a broadleaved-deciduous tree typical of cold regions, which, if abundant, may generate vegetation structurally similar to that in the nemoral forest biome. Results in Hernández Fernández (2001) show that the qualitative bioclimatic analysis can determine some of these differences in the structure of habitat. The rodent fauna of Prince Rupert was classified as indicative of taiga biome although its climate corresponds to that of the nemoral forest biome. Nevertheless, the dominant trees in the region are coniferous (Rivas Martínez et al., 1999).

The discrepancies in the Gigny sequence might also be due to the different relationship between vegetation and climate under concentrations of atmospheric CO₂ different than the modern ones (Betts et al., 1997; Farquhar, 1997; Cowling, 1999; Cowling and Sykes, 1999; Bennett and Willis, 2000). With low levels of atmospheric CO₂ the optimum temperature for photosynthesis in C₃ plants decreases, which allows them to photosynthesize in lower temperatures (Cowling and Sykes,

Table 3
Results of the qualitative bioclimatic analysis of the rodent faunas from the European late Pleistocene

Assemblage	Qualitative bioclimatic model				Quantitative bioclimatic models		
	highest probability climate zone	P_1	2nd highest probability climate zone	P_2	Walter	Köppen	Rivas Martínez
La Chênélaz 1	VI	1.000	VIII	<0.001	VI	Cfb	Mon-Hhu
La Chênélaz 2a	VI	1.000	VIII	<0.001	VI	Cfb	Mon-Hhu
La Chênélaz 2b	VI	1.000	VIII	<0.001	VI	Cfb	Mon-Hhu
La Chênélaz 2c	VI	1.000	VIII	<0.001	VI	Cfb	Mon-Hhu
La Chênélaz 4b	VI	1.000	VIII	<0.001	VI	Cfb	Mon-Hhu
La Chênélaz 4c	VI	1.000	VIII	<0.001	VI	Cfb	Mon-Hhu
La Chênélaz Ens. 4	VI	0.999	VIII	0.001	VI	Dfb	Sal
La Chênélaz 5a	VI	1.000	VIII	<0.001	VI	Cfb	Mon-Hhu
La Chênélaz 5b	VI	1.000	VIII	<0.001	VI	Cfb	Mon-Hhu
La Chênélaz 6a	VI	1.000	VIII	<0.001	VI	Cfb	Mon-Hhu
La Chênélaz 6b	VI	1.000	VIII	<0.001	VI	Cfb	Mon-Hhu
La Chênélaz 6c	VI	1.000	VIII	<0.001	VI	Cfb	Mon-Hhu
Gigny V	VI	1.000	VIII	<0.001	VI	Dfb	Mon/Sal
Gigny VI1	VI	0.999	VIII	0.001	VI/VIII	Dfb	Mbo
Gigny VI2	VI	0.875	IX	0.125	VIII	Dfc	Mbo
Gigny VI3	VI	0.989	VIII	0.011	VI/VIII	Dfb	Mbo
Gigny VI4	VI	1.000	VIII	<0.001	VI	Dfb	Mon/Sal
Gigny IX	VI	1.000	VIII	<0.001	VI	Dfb	Sal
Gigny X	VI	1.000	IX	<0.001	VI	Dfb	Sal
Gigny XI	VI	0.875	IX	0.115	VIII	Dfc	Mbo
Gigny XII	VI	0.996	VIII	0.002	VIII	Dfb	Mbo
Gigny XIII	VI	0.999	VIII	0.001	VI/VIII	Dfb	Mbo
Gigny XIVa	VI	0.999	VIII	0.001	VI/VIII	Dfb	Mbo
Gigny XIVb	VI	0.989	VIII	0.011	VIII	Dfc	Mbo
Gigny XV1	VIII	0.978	IX	0.012	VIII	Dfc	Sbo
Gigny XV2	IX	0.818	VIII	0.180	VIII	Dfc	Sbo
Gigny XV bottom	VIII	0.524	VI	0.476	VIII	Dfc	Mbo
Gigny XVIa top	VI	0.999	VIII	0.001	VI	Dfb	Mon/Sal
Gigny XVIa bottom	VI	1.000	VIII	<0.001	VI	Dfb	Mon/Sal
Gigny XVIb top 1	VI	1.000	VIII	<0.001	VI	Dfb	Mon/Sal
Gigny XVIb top 2	VI	1.000	VIII	<0.001	VI	Dfb	Sal
Gigny XVIb bottom 1	VI	0.916	VIII	0.084	VI/VIII	Dfc	Mbo
Gigny XVIb bottom 2	VI	0.998	VIII	0.002	VI/VIII	Dfb	Mbo
Gigny XVII top	VI	1.000	VIII	<0.001	VI	Dfb	Tbo
Gigny XVII botton	VI	0.999	VIII	0.001	VI/VIII	Dfb	Mbo
Gigny XIXa	VI	0.996	VIII	0.002	VIII	Dfc	Mbo
Gigny XIXb	VI	0.959	VIII	0.041	VI/VIII	Dfc	Mbo
Gigny XIXc1	VI	0.990	VI	0.010	VI/VIII	Dfb	Mbo
Gigny XIXc2	VI	0.959	VIII	0.041	VI/VIII	Dfc	Mbo
Gigny XX	VI	0.959	VIII	0.041	VI/VIII	Dfc	Mbo
Gigny XXII	VI	1.000	VIII	<0.001	VI	Dfb	Mon/Sal
Kemathenhöhle b'	VIII	0.999	IX	0.001	VIII	Dfc	Sbo
Kemathenhöhle b1 Low.	VIII	0.992	VI	0.008	VIII	Dfc	Mbo
Kemathenhöhle b1 Upp.	VIII	0.644	VI	0.356	VIII	Dfc	Mbo
Kemathenhöhle b2	VIII	0.644	VI	0.356	VIII	Dfc	Mbo
Kemathenhöhle c	VIII	0.992	VI	0.008	VIII	Dfc	Mbo
Kemathenhöhle d	VIII	0.992	VI	0.008	VIII	Dfc	Mbo
Kemathenhöhle e	VIII	1.000	VI	<0.001	VIII	Dfc	Mbo
Bacho Kiro 6a	VI	1.000	VIII	<0.001	VI	Dfb	Mon-Hhu
Bacho Kiro 6a/7	VI	1.000	VIII	<0.001	VI	Dfa	Mon-Hum
Bacho Kiro 7	VI	1.000	VIII	<0.001	VI	Dfb	Mon-Hum
Bacho Kiro 8	VI	1.000	VIII	<0.001	VI	Dfb	Mon/Sal-Hum
Bacho Kiro 11	VI	1.000	VIII	<0.001	VI	Dfb	Mon-Hhu
Bacho Kiro 11a	VI	1.000	VIII	<0.001	VI	Cfb	Mon-Hhu
Bacho Kiro 12	VI	1.000	VIII	<0.001	VI	Cfb	Mon-Hhu
Bacho Kiro 12/13	VI	1.000	VIII	<0.001	VI	Dfb	Mon-Hhu
Bacho Kiro 13	VI	1.000	VIII	<0.001	VI	Dfb	Mon-Hum
Bacho Kiro 13/13h	VI	1.000	VIII	<0.001	VI	Dfb	Mon/Sal
Karlukovo Cave 15-1	VI	1.000	VII	<0.001	VI	Csb	Mon-Hum
Karlukovo Cave 15-2	VI	1.000	VII	<0.001	VI	Csb	Mon-Hum

(continued on next page)

Table 3 (continued)

Assemblage	Qualitative bioclimatic model				Quantitative bioclimatic models		
	highest probability climate zone	P_1	2nd highest probability climate zone	P_2	Walter	Köppen	Rivas Martínez
Karlukovo Cave 16-I	VI	0.951	VII	0.049	VI	Csb	Mon-Hum
Karlukovo Cave 16-II	VI	1.000	VII	<0.001	VI	Dsb	Mon-Hum
Karlukovo Cave 16-III	VI	1.000	VII	<0.001	VI	Cfb	Mon-Hhu
Karlukovo Cave 16-IV	VI	1.000	VII	<0.001	VI	Cfb	Mon-Hhu
Karlukovo Cave 16-V	VI	0.997	VII	0.003	VI	Dsb	Mon-Hum
Karlukovo Cave 16-VI	VI	1.000	VII	<0.001	VI	Cfb	Mon-Hum
Karlukovo Cave 16-VII	VI	1.000	VII	<0.001	VI	Cfb	Mon-Hhu
Karlukovo Cave 16-VIII	VI	1.000	VII	<0.001	VI	Cfb	Mon-Hhu
Karlukovo Cave 16-IX	VI	1.000	VII	<0.001	VI	Cfb	Mon-Hum
Karlukovo Cave 16-X	VI	1.000	VII	<0.001	VI	Cfb	Mon-Hhu
Karlukovo Cave 16-XI	VI	1.000	VII	<0.001	VI	Cfb	Mon-Hhu
Karlukovo Cave 16-XII	VI	1.000	VII	<0.001	VI	Cfb	Mon-Hhu

The climatic assignments determined from climatic data estimated by the quantitative bioclimatic models are also included.

Note. For the determination of the climates according to the climatic typologies by Walter, Köppen, and Rivas Martínez we have used, respectively, Allué Andrade (1990) and Walter (1970), Strahler and Strahler (1987), and Rivas Martínez (1994). P_1 , probability of the highest probability climate zone; P_2 , probability of the second highest probability climate zone (see Hernández Fernández and Peláez-Campomanes, 2003). VI, typical temperate climate zone (nemoral broadleaved-deciduous forest biome); VIII, cold-temperate climate zone (taiga biome); IX, arctic climate zone (tundra biome). Mon, Montane; Sal, Subalpine; Tbo, Termoboreal; Mbo, Mesoboreal; Sbo, Supraboreal; Hum, Humid; Hhu, Hyperhumid.

1999). In this way, “thermophilous” vegetation could persist in an area when global temperature decreased as long as the atmospheric CO₂ concentration also decreased. Therefore, during most of the Würmian Glaciation, a period with low levels of atmospheric CO₂ (Barnola et al., 1987; Neftel et al., 1988; Crowley and North, 1991), broadleaved-deciduous forest might have persisted even if the climatic values correspond to those of taiga.

An additional effect of the lower levels of atmospheric CO₂ is the decrease in water use efficiency in C₃ plants (Cowling, 1999; Cowling and Sykes, 1999). This leads to the occurrence of more xerophilous formations during the periods with lower levels of atmospheric CO₂ than in modern times, under the same climatic conditions. This effect might be responsible for Gigny XV2 being placed within the range of the cold taiga (biome VIII) as a function of its climatic values, while it is classified as tundra (biome IX) by qualitative analysis. Tundra is usually considered to be a more xeric environment than taiga (Cowling, 1999). Since vegetation physiognomy can be partly decoupled from climate, the dominant vegetation during the glacial periods may have included, besides typical tundra species, a high percentage of species that are not found in the modern tundra biome. In particular, note the presence of *Artemisia*, a taxon that is recorded with high pollen values in the glacial periods detected in La Grande Pile and Les Echets (Woillard, 1979; de Beaulieu and Reille, 1984). This mixture of xerophilous and tundra vegetation has stimulated the definition of a new ecosystem: the “steppe-tundra” (Adams et al., 1990; Zimov et al., 1995). According to Prentice et al. (1993), this ecosystem would form an ecotone between the tundra and steppe biomes (VII/IX), which is greatly reduced today. It only persists as azonal vegetation in some mountainous areas of northwestern North America (Lloyd et al., 1994), northeastern Siberia (Yurtsev, 1982) and Tibet (Guiot et al., 1993), where drought-tolerant steppe and tundra taxa are found together.

During the studied period, there is a correlation between temperature and concentration of atmospheric CO₂ (Crowley and North, 1991). Therefore, if the effects of atmospheric CO₂ levels were in fact responsible for the inconsistencies between the qualitative and quantitative approaches of the bioclimatic analysis, we would expect that those levels that give inconsistent results should be the ones with the lowest temperatures (and low levels of atmospheric CO₂). The Gigny levels were divided into three groups: those that were consistently classified by the qualitative and quantitative analysis, those that were inconsistently classified, and those that the quantitative analysis placed in an ecotone, which cannot be determined by the qualitative analysis. One-way ANOVA was performed on the mean annual temperature in each of these three groups to determine whether the inconsistent results produced significantly lower temperatures than the other groups. This analysis was restricted to Gigny in order to avoid problems derived from the mixture of data from different geographical areas (at different latitudes the temperature is different although the CO₂ levels are the same). The results indicate highly significant differences in temperature between the levels with consistent and inconsistent climatic classifications; the inconsistent levels had significantly lower temperatures than the levels consistently classified or the levels classified as an ecotone (Fig. 7), thus supporting the hypothesis regarding the influence of atmospheric CO₂ concentration on the internal consistency of the bioclimatic analysis.

Comparison with previous paleoclimatic analyses

Quantitative climatic analyses

The sequence of mammal assemblages from Karlukovo was studied by Popov et al. (1994), who established a paleotem-

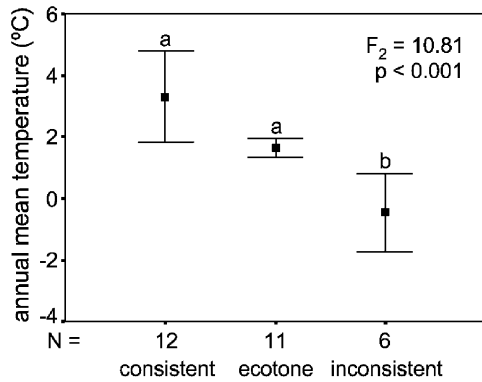


Figure 7. Effect of mean annual temperature (mean \pm 95% confidence interval), as a surrogate for atmospheric CO₂ concentration, on the consistency of the climatic classification of Gigny levels between the qualitative and the quantitative bioclimatic analysis. *P* value from the one-way ANOVA for the 29 levels studied (*N*, number of levels). Lower-case letters indicate homogeneous subsets calculated by post hoc Tukey's test; groups of levels are significantly different when they do not share the same letter.

perature curve that coincides in essence with the one presented here. They also showed that aridity increases to the end of the sequence.

Chaline et al. (1995) and Montuire et al. (1997) performed paleoclimatic analyses of the rodent faunas from Gigny, but some of their climatic inferences are neither self-consistent nor in agreement with the results presented here. This may be due to the difficulties in the interpretation of the results of their methods. Montuire et al. (1997) studied the paleoclimate of Gigny by applying a method based on the species richness of Arvicolidae in the rodent faunas. This method involves making a simple linear regression where the dependent variable is mean annual temperature and the independent variable is the number of arvicolid species in the assemblage. The results of this test were satisfactory in modern faunas ($r^2 = 0.85$; SE = $\pm 3.74^\circ\text{C}$), but to apply this method to the fossil record may be difficult because the fossil associations generally do not register all the species that were living in the paleocommunity. Therefore, any results using exclusively the species richness in fossil assemblages to infer climate must be very cautious in its methodological layout and conclusions and should be considered tentative. Nieto and Rodríguez (2003) also point out flaws in this methodology. Chaline et al. (1995) used principal components analysis (PCA) to analyze the relative abundances of the different rodent species recorded in each level at Gigny. The environmental and climatic interpretation of the axes derived from this multivariate analysis is based on the study of the ecological requirements of the taxa with higher influence on each axis. This interpretation is complex and cannot easily be examined in terms of concrete climatic factors because each species is affected by the different climatic variables as a whole. Furthermore, Chaline et al. (1995) did not include in the PCA modern faunal associations with known climatic conditions, which would have allowed for a more straightforward climatic interpretation of the results (Hernández Fernández et al., 2003, in press; Hernández Fernández and Vrba, in press).

On the other hand, Campy et al. (1989) and Chaline et al. (1995) also applied a method developed by Hokr (1951) to the rodent associations of Gigny, which provided temperature estimations and a trend during the studied periods similar to the ones provided by the quantitative bioclimatic analysis presented here. Hokr's method uses the knowledge about the climatic distributions of modern species to infer the climate of a fossil site. Its results, as in the bioclimatic analysis, are directly interpretable as climatic factors.

Recently, Navarro et al. (2004) have studied the isotopic composition of arvicoline teeth from Gigny. Although there is no significant correlation between the $\delta^{18}\text{O}$ values presented by these authors and the mean annual temperature or the temperature of the coldest month reported here (respectively, $r = -0.298$, $P = 0.123$; $r = -0.083$, $P = 0.676$), there is a highly significant correlation with the temperature of the warmest month ($r = -0.510$, $P = 0.006$). This may be related with the fact that arvicoline species show outdoor activity greater from spring to fall than during winter. Consequently, the probability of capture by owls, mainly responsible for accumulation of fossil rodent assemblages, is higher during summer (Navarro et al., 2004). Therefore, the isotopic record in dental tissue is most probably related to summer temperatures.

Although the levels sampled do not match exactly, the paleoecological analysis of bird assemblages from Gigny (Campy et al., 1989) also shows similarity to the results presented here.

Let us compare the Gigny paleoclimatic results presented here with the ones estimated for La Grande Pile, which has a comprehensive and nearby palynological record of the last interglacial–glacial cycle (Woillard and Mook, 1982; de Beaulieu and Reille, 1992). The paleoclimatic interpretation of La Grande Pile (Guiot et al., 1989; Guiot, 1990; Guiot et al., 1993) generated estimates of mean annual temperature for the Würm glacial age that are higher than those produced by the quantitative bioclimatic analysis. Nevertheless, for the Eemian these estimations are not dissimilar. Palynological data from La Grande Pile show very low precipitation during the Würmian (until 800 mm lower than today). During the Eemian, however, they give values similar to today's, which coincides with the results of the bioclimatic analysis. The discrepancies between the two analyses are easily explained by the differences in atmospheric CO₂ levels during the cold periods. As noted above, low CO₂ levels led to a diminishing of the water use efficiency in C₃ plants and allow plants to photosynthesize at lower temperatures (Cowling, 1999; Cowling and Sykes, 1999). This generates, under similar climatic conditions, the occurrence of more xeric and thermophilous vegetation formations, which may produce mistaken climatic inferences if we only take into account vegetation bioindicators (Cowling, 1999). During interglacial periods, CO₂ levels are similar to the modern ones (Crowley and North, 1991) and, hence, there are no discrepancies between the results of the two methodologies. Despite the differences between the estimates from pollen and rodents, precipitation and temperature show a parallel trend in both data sets: there is higher precipitation during the warm periods than during the cold ones (Guiot, 1990).

Guiot et al. (1993) attributed the high estimations of temperature for the Würm glaciation to the scarcity of modern vegetation analogues with which to compare the palynological associations. The closest analogues were those from the warm steppe. In order to solve this difficulty, they developed new methodologies to select modern analogues by the study of other evidence, like inferred biome and occurring fossil insect associations. In these cases, the temperature estimates from Guiot et al. (1993) match the ones from the quantitative bioclimatic analysis.

Recently, Fauquette et al. (1999) applied a different methodology to the palynological data of La Grande Pile. Instead of looking for modern analogues for the plant paleocommunities, they studied the climatic constraints of each species occurring in them. From these, they calculated a climatic range in which theoretically all the taxa in a paleocommunity could live. Their results show a paleotemperature curve that largely agrees with the one provided by the quantitative bioclimatic analysis of the rodent faunas from Gigny. Nevertheless, their estimation of precipitation shows lower values during the coldest periods, although it illustrates a similar trend. Again, the observed differences may be attributed to the decrease in water efficiency in C_3 plants under conditions of low concentration of atmospheric CO_2 .

Fossil coleopteran associations of La Grande Pile have also provided estimations of the mean temperature of the coldest and warmest months (Ponel, 1995), which are consistent with the temperatures estimated here for Gigny.

Qualitative climatic analyses

Fauquette et al. (1999) also reconstructed the biomes in the area close to La Grande Pile during the last interglacial–glacial cycle, based on the pollen record of this sequence and the structure of plant functional types inferable from it. The comparison of their results with the ones offered by the qualitative bioclimatic analysis, however, is difficult for two reasons. First, the biome typology they have used is different from the one employed here. Second, they do not provide a time scale for their reconstruction of the paleovegetation. Nevertheless, that reconstruction shows biomes that are analogues to the ones inferred here from the micromammalian evidence. The biggest difference between the analyses is that Fauquette et al. (1999) inferred the presence of cold steppes during most of the middle Würm (OIS 3) and identified some episodes of taiga and tundra. These discrepancies may be due to methodological differences in biome inference. For example, neither the qualitative bioclimatic analysis nor Fauquette et al.'s (1999) method can distinguish ecotonal situations between biomes. The bioclimatic analysis may classify a forest-steppe (ecotones VI/VII or VII/VIII) assemblage as belonging to the broadleaved-deciduous forest (VI), steppe (VII) or taiga (VIII) biomes, depending on those ecosystemic factors that may affect the mammal communities, probably the density of tree cover or the dominant tree species. In the same way, the biome reconstruction method used by Fauquette et al. (1999) may

indicate the presence of the steppe biome due to the great abundance of pollen from steppe herbaceous species in these ecotonal regions. Recently, Willis et al. (2000, 2001), Carcaillet and Vernet (2001) and Willis and van Andel (2004) showed convincing evidence for the continuous presence of tree vegetation during full-glacial periods throughout central and eastern Europe.

An alternative way of interpreting these ecotonal situations from the results of the qualitative bioclimatic analysis might be to study the probabilities of the inferred most probable and second most probable climate zones (P_1 and P_2 in Table 3). Then, a potential ecotone between broadleaved-deciduous forest and tundra (VI/IX), which does not exist today, could be suggested for Gigny XI (P_1 is relatively low, 0.875). Nevertheless, this alternative method of interpretation must be thoroughly tested before trying to apply it.

Concluding remarks

The use of independent methodologies of paleoecological analysis is essential when attempting to reconstruct paleoenvironments, and major benefits can be obtained by using the paleoclimatic evidence provided by the mammalian fossil record. Results of this work indicate that bioclimatic analysis of fossil rodent faunas provides an independent, efficient and robust assessment of continental Pleistocene climate. This method, based on studies of extant mammal communities, consist of two complementary procedures (qualitative and quantitative), which provide information on both the physiognomy of the biome and the climatic values under which the studied community lived, and thus allows a parallel approach to the reconstruction of paleoenvironments. Comparison of the results obtained from both models have provided further evidence on the close coupling between mammalian faunas, vegetation, and climate, allowing for the influence of atmospheric CO_2 levels on the climate–vegetation relationship. Particularly, the sequences studied here from central and eastern Europe provide a high-temporal-resolution record of climatic change, which can be correlated with palynological data and with the global oxygen isotope record. Nevertheless, the results offered by the quantitative bioclimatic analysis should not be perceived as absolute numbers. Instead, they should be seen as indicators of general geographical and temporal trends. Additional successions of rodent faunas in other parts of Europe, specially the Mediterranean, are needed to test the general spatial and chronological patterns presented here on biome and climate change in the European late Pleistocene.

Acknowledgments

I am indebted to M.A. Álvarez Sierra and P. Peláez-Campomanes for their kind advice, valuable suggestions and constructive comments on previous drafts of this paper. M. Jeannet kindly provided numerical information about the fossiliferous levels of La Chênélaz. B. Luna helped with the statistical analysis. W.A. Green is thanked for his useful

observations and assistance with the English of the original manuscript. Nieves López Martínez, Robert A. Martin and Sophie Montuire provided helpful comments on the manu-

script. Projects PB98-0691-C03-02 and BTE2002-00410, sponsored by the Spanish CICYT and MCYT, respectively, funded this study.

Appendix A. Bioclimatic spectra of the European rodent fossil assemblages used in this work

Assemblage	I	II	II/III	III	IV	V	VI	VII	VIII	IX
La Chênélaz 1	1.693	1.693	1.693	1.693	13.915	1.693	57.249	2.407	16.296	1.667
La Chênélaz 2a	1.814	1.814	1.814	1.814	10.743	1.814	59.552	2.579	15.675	2.381
La Chênélaz 2b	0.000	0.000	0.000	0.000	10.417	0.000	68.750	6.250	14.583	0.000
La Chênélaz 2c	0.000	0.000	0.000	0.000	13.889	0.000	62.037	2.778	17.593	3.704
La Chênélaz 4b	0.000	0.000	0.000	0.000	12.500	0.000	62.500	6.250	12.500	6.250
La Chênélaz 4c	0.000	0.000	0.000	0.000	20.000	0.000	60.000	5.000	10.000	5.000
La Chênélaz Ens. 4	0.000	0.000	0.000	0.000	9.259	0.000	44.444	8.333	27.778	10.185
La Chênélaz 5a	0.000	0.000	0.000	0.000	16.667	0.000	51.515	6.818	19.697	5.303
La Chênélaz 5b	0.000	0.000	0.000	0.000	13.636	0.000	57.576	6.818	16.667	5.303
La Chênélaz 6a	0.000	0.000	0.000	0.000	15.000	0.000	58.333	7.500	13.333	5.833
La Chênélaz 6b	1.190	1.190	1.190	1.190	13.690	1.190	56.944	7.440	11.111	4.861
La Chênélaz 6c	0.000	0.000	0.000	0.000	13.095	0.000	58.333	8.929	15.476	4.167
Gigny V	0.000	0.000	0.000	0.000	16.667	0.000	38.889	9.722	19.444	15.278
Gigny VI 1	0.000	0.000	0.000	0.000	10.000	0.000	36.667	11.667	23.333	18.333
Gigny VI 2	0.000	0.000	0.000	0.000	4.167	0.000	26.389	26.389	15.278	27.778
Gigny VI 3	0.000	0.000	0.000	0.000	8.333	0.000	38.889	9.722	27.778	15.278
Gigny VI 4	0.000	0.000	0.000	0.000	11.905	0.000	38.095	22.619	19.048	8.333
Gigny IX	0.000	0.000	0.000	0.000	14.815	0.000	40.741	6.481	20.370	17.593
Gigny X	0.000	0.000	0.000	0.000	11.667	0.000	38.333	11.667	11.667	26.667
Gigny XI	0.000	0.000	0.000	0.000	7.143	0.000	33.333	8.333	23.810	27.381
Gigny XII	0.000	0.000	0.000	0.000	3.571	0.000	29.762	22.619	20.238	23.810
Gigny XIII	0.000	0.000	0.000	0.000	9.375	0.000	38.542	7.292	23.958	20.833
Gigny XIVa	0.000	0.000	0.000	0.000	8.333	0.000	34.259	17.593	21.296	18.519
Gigny XIVb	0.000	0.000	0.000	0.000	3.125	0.000	32.292	19.792	23.958	20.833
Gigny XV 1	0.000	0.000	0.000	0.000	3.571	0.000	29.762	8.333	34.524	23.810
Gigny XV 2	0.000	0.000	0.000	0.000	4.167	0.000	26.389	9.722	31.944	27.778
Gigny XV bottom	0.000	0.000	0.000	0.000	9.375	0.000	32.292	7.292	30.208	20.833
Gigny XVIa top	0.000	0.000	0.000	0.000	11.364	0.000	32.576	28.030	21.970	6.061
Gigny XVIa bottom	0.000	0.000	0.000	0.000	10.417	0.000	38.194	25.694	20.139	5.556
Gigny XVIb top 1	0.000	0.000	0.000	0.000	12.179	0.000	37.821	26.282	18.590	5.128
Gigny XVIb top 2	0.000	0.000	0.000	0.000	8.333	0.000	39.815	23.148	21.296	7.407
Gigny XVIb bottom 1	0.000	0.000	0.000	0.000	2.778	0.000	37.963	17.593	30.556	11.111
Gigny XVIb bottom 2	0.000	0.000	0.000	0.000	2.778	0.000	39.815	23.148	26.852	7.407
Gigny XVII top	0.000	0.000	0.000	0.000	9.375	0.000	36.458	19.792	21.875	12.500
Gigny XVII bottom	0.000	0.000	0.000	0.000	2.778	0.000	37.963	23.148	25.000	11.111
Gigny XIXa	0.000	0.000	0.000	0.000	3.571	0.000	29.762	22.619	20.238	23.810
Gigny XIXb	0.000	0.000	0.000	0.000	4.167	0.000	43.056	9.722	31.944	11.111
Gigny XIXc1	0.000	0.000	0.000	0.000	3.571	0.000	36.905	22.619	27.381	9.524
Gigny XIXc2	0.000	0.000	0.000	0.000	4.167	0.000	43.056	9.722	31.944	11.111
Gigny XX	0.000	0.000	0.000	0.000	4.167	0.000	43.056	9.722	31.944	11.111
Gigny XXII	0.000	0.000	0.000	0.000	12.500	0.000	40.833	15.833	24.167	6.667
Kemathenhöhle b'	0.000	0.000	0.000	0.000	6.250	0.000	22.917	7.292	39.583	23.958
Kemathenhöhle b1 Low.	0.000	0.000	0.000	0.000	8.333	0.000	21.667	19.167	31.667	19.167
Kemathenhöhle b1 Upp.	0.000	0.000	0.000	0.000	6.944	0.000	30.556	15.972	30.556	15.972
Kemathenhöhle b2	0.000	0.000	0.000	0.000	6.944	0.000	30.556	15.972	30.556	15.972
Kemathenhöhle c	0.000	0.000	0.000	0.000	8.333	0.000	21.667	19.167	31.667	19.167
Kemathenhöhle d	0.000	0.000	0.000	0.000	8.333	0.000	21.667	19.167	31.667	19.167
Kemathenhöhle e	0.000	0.000	0.000	0.000	5.000	0.000	23.333	15.833	36.667	19.167
Bacho Kiro 6a	0.000	0.000	0.000	0.000	13.889	0.000	43.056	24.306	16.667	2.083
Bacho Kiro 6a/7	0.000	0.000	0.000	0.000	12.821	0.000	42.308	22.436	17.949	4.487
Bacho Kiro 7	0.000	0.000	0.000	0.000	11.111	0.000	38.889	29.861	15.278	4.861
Bacho Kiro 8	0.000	0.000	0.000	0.000	11.667	0.000	41.667	24.167	20.000	2.500
Bacho Kiro 11	0.000	0.000	0.000	0.000	12.821	0.000	43.590	26.282	15.385	1.923
Bacho Kiro 11a	0.000	0.000	0.000	0.000	13.889	0.000	47.222	20.139	16.667	2.083
Bacho Kiro 12	0.000	0.000	0.000	0.000	10.417	0.000	47.917	27.604	12.500	1.563
Bacho Kiro 12/13	0.000	0.000	0.000	0.000	12.821	0.000	43.590	26.282	15.385	1.923
Bacho Kiro 13	0.000	0.000	0.000	0.000	11.111	0.000	40.278	29.861	16.667	2.083
Bacho Kiro 13/13h	0.000	0.000	0.000	0.000	10.000	0.000	40.000	27.500	20.000	2.500
Karlukovo Cave 15-1	0.000	0.000	0.000	0.000	14.583	0.000	43.750	37.500	2.083	2.083

(continued on next page)

Appendix A (continued)

Assemblage	I	II	II/III	III	IV	V	VI	VII	VIII	IX
Karlukovo Cave 15-2	0.000	0.000	0.000	0.000	15.385	0.000	46.154	32.692	3.846	1.923
Karlukovo Cave 16-I	0.000	0.000	0.000	0.000	13.095	0.000	34.524	45.238	3.571	3.571
Karlukovo Cave 16-II	0.000	0.000	0.000	0.000	9.722	0.000	38.889	39.583	6.944	4.861
Karlukovo Cave 16-III	0.000	0.000	0.000	0.000	11.667	0.000	46.667	34.167	5.000	2.500
Karlukovo Cave 16-IV	0.000	0.000	0.000	0.000	13.889	0.000	47.222	26.389	8.333	4.167
Karlukovo Cave 16-V	0.000	0.000	0.000	0.000	8.333	0.000	36.905	44.643	5.952	4.167
Karlukovo Cave 16-VI	0.000	0.000	0.000	0.000	9.722	0.000	55.556	28.472	4.167	2.083
Karlukovo Cave 16-VII	0.000	0.000	0.000	0.000	8.974	0.000	51.282	33.974	3.846	1.923
Karlukovo Cave 16-VIII	0.000	0.000	0.000	0.000	7.778	0.000	47.778	39.444	3.333	1.667
Karlukovo Cave 16-IX	0.000	0.000	0.000	0.000	9.722	0.000	55.556	28.472	4.167	2.083
Karlukovo Cave 16-X	0.000	0.000	0.000	0.000	7.778	0.000	47.778	35.000	5.556	3.889
Karlukovo Cave 16-XI	0.000	0.000	0.000	0.000	8.974	0.000	51.282	33.974	3.846	1.923
Karlukovo Cave 16-XII	0.000	0.000	0.000	0.000	8.333	0.000	51.190	30.357	5.952	4.167

Appendix B. Values for the different climatic factors (see Table 2) estimated by applying the quantitative bioclimatic models to the late Pleistocene European rodent faunas

Assemblage	T (°C)	Tp (0.1°C)	Tmax (°C)	Tmin (°C)	Mta (°C)	It (0.1°C)	Itc (0.1°C)	VAP (months)	FVAP (months)	P (mm)	D (months)
La Chênélaz 1	9.9	1116	17.8	3.0	14.8	159	120	7.0	7.1	1432	-0.2
La Chênélaz 2a	9.8	1080	17.3	3.2	14.0	162	112	6.8	7.3	1511	-0.6
La Chênélaz 2b	9.4	928	16.8	3.1	13.7	156	89	6.4	7.6	1629	-1.4
La Chênélaz 2c	8.1	921	16.3	1.0	15.3	102	60	6.3	7.0	1453	-0.9
La Chênélaz 4b	8.5	919	16.0	2.1	13.8	128	62	6.2	7.0	1499	-0.9
La Chênélaz 4c	10.1	1058	17.2	4.1	13.1	182	107	6.9	6.9	1418	-0.1
La Chênélaz Ens. 4	3.0	721	14.9	-8.3	23.1	-135	-65	4.9	5.3	1029	-0.5
La Chênélaz 5a	7.0	933	16.8	-1.9	18.6	32	39	6.2	6.1	1189	-0.1
La Chênélaz 5b	7.6	912	16.3	-0.1	16.4	75	47	6.1	6.6	1358	-0.6
La Chênélaz 6a	8.4	954	16.5	1.4	15.1	112	65	6.3	6.7	1386	-0.4
La Chênélaz 6b	9.8	1078	17.3	3.4	13.9	166	107	6.8	6.8	1431	-0.2
La Chênélaz 6c	8.0	925	16.6	0.4	16.2	88	58	6.2	6.7	1380	-0.6
Gigny V	4.3	848	15.2	-5.8	21.0	-73	-36	5.4	4.7	920	0.6
Gigny VI 1	2.0	696	13.9	-9.4	23.2	-167	-102	4.5	4.3	885	0.1
Gigny VI 2	0.2	598	12.6	-11.7	24.2	-232	-161	3.6	3.0	731	0.6
Gigny VI 3	1.6	663	14.0	-10.3	24.2	-190	-107	4.4	4.6	916	-0.3
Gigny VI 4	4.8	851	16.8	-6.8	23.5	-87	-14	5.5	4.8	907	0.6
Gigny IX	3.7	792	14.3	-6.2	20.4	-86	-59	5.1	4.8	972	0.2
Gigny X	3.1	736	12.8	-5.5	18.2	-78	-92	4.6	4.2	992	0.2
Gigny XI	-0.3	569	11.6	-11.5	23.1	-234	-174	3.6	3.7	840	-0.2
Gigny XII	0.1	584	12.8	-12.2	25.0	-242	-157	3.7	3.5	780	0.2
Gigny XIII	1.5	657	13.0	-9.3	22.3	-171	-119	4.3	4.4	935	-0.3
Gigny XIVa	1.9	689	14.1	-9.8	23.9	-178	-104	4.4	4.1	846	0.2
Gigny XIVb	0.1	574	13.1	-12.5	25.6	-250	-154	3.7	3.8	816	-0.1
Gigny XV 1	-2.5	466	11.6	-16.4	28.0	-352	-218	3.1	3.5	712	-0.5
Gigny XV 2	-2.9	460	11.2	-16.6	27.7	-361	-233	3.0	3.1	653	-0.2
Gigny XV bottom	-0.2	609	13.0	-12.8	25.8	-259	-155	4.0	3.9	760	0.0
Gigny XVIa top	4.1	844	17.5	-9.2	26.6	-142	-23	5.4	4.4	761	1.0
Gigny XVIa bottom	4.9	847	17.2	-7.3	24.5	-97	-9	5.5	4.8	903	0.6
Gigny XVIb top 1	5.5	889	17.6	-6.5	24.1	-75	8	5.7	4.9	894	0.8
Gigny XVIb top 2	4.2	791	16.4	-7.8	24.2	-113	-31	5.2	4.9	949	0.2
Gigny XVIb bottom 1	0.9	603	14.5	-12.5	27.0	-241	-118	4.1	4.6	895	-0.5
Gigny XVIb bottom 2	2.4	667	15.6	-10.7	26.3	-191	-78	4.5	4.8	947	-0.3
Gigny XVII top	3.1	754	15.4	-8.9	24.2	-146	-64	4.9	4.5	876	0.3
Gigny XVII bottom	1.9	649	14.9	-10.9	25.8	-198	-94	4.4	4.6	921	-0.3
Gigny XIXa	0.1	584	12.8	-12.2	25.0	-242	-157	3.7	3.5	780	0.2
Gigny XIXb	1.3	608	14.1	-11.2	25.2	-211	-112	4.2	5.0	1001	-0.9
Gigny XIXc1	1.8	656	15.3	-11.6	26.9	-214	-93	4.4	4.5	878	-0.2
Gigny XIXc2	1.3	608	14.1	-11.2	25.2	-211	-112	4.2	5.0	1001	-0.9
Gigny XX	1.3	608	14.1	-11.2	25.2	-211	-112	4.2	5.0	1001	-0.9
Gigny XXII	4.5	831	16.6	-7.3	23.8	-101	-20	5.4	5.1	940	0.3
Kemathenhöhle b'	-3.7	464	11.9	-19.1	30.9	-418	-239	3.0	3.0	518	0.0

Appendix B (continued)

Assemblage	T (°C)	Tp (0.1°C)	Tmax (°C)	Tmin (°C)	Mta (°C)	It (0.1°C)	Itc (0.1°C)	VAP (months)	FVAP (months)	P (mm)	D (months)
Kemathenhöhle b1 Low.	0.1	619	14.1	-13.8	27.9	-275	-140	4.0	3.8	716	0.1
Kemathenhöhle b1 Upp.	-1.2	604	14.0	-16.4	30.3	-340	-170	3.8	3.0	505	0.7
Kemathenhöhle b2	0.1	619	14.1	-13.8	27.9	-275	-140	4.0	3.8	716	0.1
Kemathenhöhle c	-1.2	604	14.0	-16.4	30.3	-340	-170	3.8	3.0	505	0.7
Kemathenhöhle d	-1.2	604	14.0	-16.4	30.3	-340	-170	3.8	3.0	505	0.7
Kemathenhöhle e	-2.5	516	13.2	-18.2	31.4	-389	-203	3.4	3.1	535	0.2
Bacho Kiro 6a	7.0	954	10.3	-3.9	22.2	-8	48	6.2	5.4	1010	0.7
Bacho Kiro 6a/7	6.2	907	17.5	-4.9	22.4	-36	23	5.9	5.3	997	0.6
Bacho Kiro 7	6.1	904	17.8	-5.5	20.4	-49	20	5.8	4.9	938	0.9
Bacho Kiro 8	5.9	893	17.8	-5.8	23.6	-58	20	5.8	5.3	972	0.5
Bacho Kiro 11	7.2	951	18.3	-3.7	21.9	-1	51	6.2	5.5	1033	0.7
Bacho Kiro 11a	7.4	952	18.0	-2.8	20.7	19	54	6.2	5.8	1107	0.4
Bacho Kiro 12	7.8	943	18.1	-2.2	20.3	35	61	6.2	5.8	1157	0.3
Bacho Kiro 12/13	7.2	951	18.3	-3.7	21.9	-1	51	6.2	5.5	1033	0.7
Bacho Kiro 13	6.4	917	18.3	-5.4	23.6	-43	33	5.9	5.1	957	0.8
Bacho Kiro 13/13h	5.5	871	17.9	-6.7	24.5	-79	11	5.7	5.1	941	0.6
Karlukovo Cave 15-1	9.9	1084	19.5	0.7	18.8	113	115	6.8	5.5	1092	1.4
Karlukovo Cave 15-2	9.9	1081	19.3	1.0	18.2	120	115	6.9	5.7	1136	1.2
Karlukovo Cave 16-I	8.4	1043	19.6	-2.7	22.3	30	81	6.5	4.6	880	1.9
Karlukovo Cave 16-II	7.4	953	18.4	-3.4	21.8	7	51	6.0	4.9	983	1.2
Karlukovo Cave 16-III	9.1	1014	18.7	-0.1	18.8	90	91	6.5	5.6	1160	0.8
Karlukovo Cave 16-IV	8.6	1001	18.1	-0.4	18.5	77	77	6.4	5.7	1151	0.7
Karlukovo Cave 16-V	7.4	950	18.7	-3.9	22.7	-5	51	6.0	4.7	946	1.3
Karlukovo Cave 16-VI	9.8	993	18.1	2.2	15.9	142	101	6.5	6.4	1378	0.1
Karlukovo Cave 16-VII	9.4	989	18.4	0.9	17.5	113	95	6.4	6.0	1283	0.4
Karlukovo Cave 16-VIII	9.1	981	18.7	-0.2	18.9	88	89	6.3	5.7	1208	0.6
Karlukovo Cave 16-IX	9.8	993	18.1	2.2	15.9	142	101	6.5	6.4	1378	0.1
Karlukovo Cave 16-X	8.3	942	18.0	-0.9	18.9	65	66	6.1	5.6	1203	0.4
Karlukovo Cave 16-XI	9.4	989	18.4	0.9	17.5	113	95	6.4	6.0	1283	0.4
Karlukovo Cave 16-XII	8.6	941	17.7	0.0	17.6	86	70	6.2	5.9	1279	0.2

References

- Adams, J.M., Faure, H., Faure-Denard, L., McGlade, J.M., Woodward, F.I., 1990. Increases in terrestrial carbon storage from the Last Glacial Maximum to the present. *Nature* 348, 711–714.
- Allué Andrade, J.L., 1990. Atlas Fitoclimático de España. Monografías INIA 69, 1–223.
- Arléry, R., 1970. The climate of France, Belgium, The Netherlands and Luxembourg. In: Wallén, C.C. (Ed.), *Climates of Northern and Western Europe*, World Survey of Climatology, vol. 5. Elsevier, Amsterdam, pp. 119–158.
- Barnola, J.M., Raynaud, D., Korotkevich, Y.S., Lorius, C., 1987. Vostok ice core provides 160,000-year record of atmospheric CO₂. *Nature* 329, 408–414.
- Barron, E., Pollard, D., 2002. High-resolution climate simulations of Oxygen Isotope Stage 3 in Europe. *Quaternary Research* 58, 296–309.
- Bennett, K.D., Willis, K.J., 2000. Effect of global atmospheric carbon dioxide on glacial–interglacial vegetation change. *Global Ecology and Biogeography* 9, 355–361.
- Betts, R.A., Cox, P.M., Lee, S.E., Woodward, F.I., 1997. Contrasting physiological and structural vegetation feedbacks in climate change simulations. *Nature* 387, 796–799.
- Broccoli, A.J., Manabe, S., 1987. The influence of continental ice, atmospheric CO₂, and land albedo on the climate of the last glacial maximum. *Climate Dynamics* 1, 87–99.
- Brunet-Lecomte, P., Nadachowski, A., Chaline, J., 1992. *Microtus (Terricola) grafi* nov. sp. du Pléistocène Supérieur de la grotte de Bacho Kiro (Bulgarie). *Geobios* 25, 505–509.
- Campy, M., Chaline, J., Vuilleme, M. (Eds.), 1989. La Baume de Gigny (Jura), Gallia Préhistoire, vol. 27. CNRS, Paris, pp. 1–263 (Supplement).
- Carcaillet, C., Vernet, J.L., 2001. Comments on “The Full-Glacial forests of Central and Southeastern Europe” by Willis et al. *Quaternary Research* 55, 385–387.
- Chaline, J., 1972. Les Rongeurs du Pléistocène moyen et supérieur de France (Systématique, Biostratigraphie, Paléoclimatologie). Cahiers de Paléontologie. CNRS, Paris.
- Chaline, J., Brunet-Lecomte, P., Campy, M., 1995. The last glacial/interglacial record of rodent remains from the Gigny karst sequence in the French Jura used for paleoclimatic and palaeoecological reconstructions. *Palaeogeography, Palaeoclimatology, Palaeoecology* 117, 229–252.
- CLIMAP Project Members, 1976. The Surface of the Ice-Age Earth. *Science* 191, 1131–1137.
- COHMAP Members, 1988. Climatic changes of the last 18,000 years: observations and model simulations. *Science* 241, 1043–1052.
- Cosgrove, B.A., Barron, E.J., Pollard, D., 2002. A simple interactive vegetation model coupled to the GENESIS GCM. *Global and Planetary Change* 32, 253–278.
- Cowling, S.A., 1999. Simulated effects of low atmospheric CO₂ on structure and composition of North America vegetation at the Last Glacial Maximum. *Global Ecology and Biogeography* 8, 81–93.
- Cowling, S.A., Sykes, M.T., 1999. Physiological significance of low atmospheric CO₂ for plant–climate interactions. *Quaternary Research* 52, 237–242.
- Crowley, T.J., North, G.R., 1991. *Paleoclimatology*. Oxford University Press and Clarendon Press, Oxford.
- Daams, R., van der Meulen, A.J., Peláez-Campomanes, P., Álvarez Sierra, M.A., 1999. Trends in rodent assemblages from the Aragonian (early–middle Miocene) of the Calatayud-Daroca Basin, Aragon, Spain. In: Agustí, J., Rook, L., Andrews, P. (Eds.), *Hominid Evolution and Climatic Change in Europe, The Evolution of Neogene Terrestrial Ecosystems in Europe*, vol. 1. Cambridge Univ. Press, Cambridge, pp. 127–139.
- Dansgaard, W., Johnsen, S.J., Clausen, H.B., Dahl-Jensen, D., Gundestrup, N.S., Hammer, C.U., Hvildberg, C.S., Steffensen, J.P., Svelnbyörnsdottir, A.E., Jouzel, J., Bond, G., 1993. Evidence for general instability of past climate from a 250-kyr ice-core record. *Nature* 364, 218–220.

- de Beaulieu, J.L., Reille, M., 1984. A long Upper Pleistocene pollen record from Les Echets, near Lyon, France. *Boreas* 13, 111–132.
- de Beaulieu, J.L., Reille, M., 1992. The last climatic cycle at la Grande Pile (Vosges, France): a new pollen profile. *Quaternary Science Reviews* 11, 431–438.
- Farquhar, G.D., 1997. Carbon dioxide and vegetation. *Science* 278, 1411.
- FAUNMAP Working Group, 1996. Spatial response of mammals to Late Quaternary environmental fluctuations. *Science* 272, 1601–1606.
- Fauquette, S., Guiot, J., Menut, M., de Beaulieu, J.-L., Reille, M., Guenet, P., 1999. Vegetation and climate since the last interglacial in the Vienne area (France). *Global and Planetary Change* 20, 1–17.
- Florineth, D., Schluchter, C., 2000. Alpine evidence for atmospheric circulation patterns in Europe during the Last Glacial Maximum. *Quaternary Research* 54, 295–308.
- Guiot, J., 1990. Methodology of the last climatic cycle reconstruction in France from pollen data. *Palaeogeography, Palaeoclimatology, Palaeoecology* 80, 49–69.
- Guiot, J., Pons, A., de Beaulieu, J.L., Reille, M., 1989. A 140,000-year continental climate reconstruction from two European pollen records. *Nature* 338, 309–313.
- Guiot, J., de Beaulieu, J.L., Cheddadi, R., David, F., Ponel, P., Reille, M., 1993. The climate in Western Europe during the last glacial/interglacial cycle derived from pollen and insect remains. *Palaeogeography, Palaeoclimatology, Palaeoecology* 103, 73–93.
- Harrison, S.P., Prentice, I.C., Bartlein, P.J., 1992. Influence of insulation and glaciation on atmospheric circulation in the North Atlantic sector: implications of general circulation model experiments for the Late Quaternary climatology of Europe. *Quaternary Science Reviews* 11, 283–299.
- Hernández Fernández, M., 2001. Bioclimatic discriminant capacity of terrestrial mammal faunas. *Global Ecology and Biogeography* 10, 113–128.
- Hernández Fernández, M., Peláez-Campomanes, P., 2003. The bioclimatic model: a method of palaeoclimatic qualitative inference based on mammal associations. *Global Ecology and Biogeography* 12, 507–517.
- Hernández Fernández, M., Peláez-Campomanes, P., 2005. Quantitative palaeoclimatic inference based on terrestrial mammal faunas. *Global Ecology and Biogeography* 14, 39–56.
- Hernández Fernández, M., Vrba, E.S., in press. Plio-Pleistocene climatic change in the Turkana Basin (East Africa): evidence from large mammal faunas. *Journal of Human Evolution*.
- Hernández Fernández, M., Salesa, M.J., Sánchez, I.M., Morales, J., 2003. Paleocología del género *Anchitherium* von Meyer, 1834 (Equidae, Perissodactyla, Mammalia) en España: evidencias a partir de la faunas de macromamíferos. *Coloquios de Paleontología, Volumen Extraordinario* 1, 253–280.
- Hernández Fernández, M., Alberdi, M.T., Azanza, B., Montoya, P., Morales, J., Nieto, M., Peláez-Campomanes, P., in press. Identification problems of arid environments in the Neogene-Quaternary mammal record of Spain. *Journal of Arid Environments*.
- Hír, J., 1993a. *Allocrietus ehiki* Schaub, 1930 (Rodentia, Mammalia) finds from Vilány 3 and Esztramos 3 (Hungary). *Fragmenta Mineralogica et Palaeontologica* 16, 61–80.
- Hír, J., 1993b. *Cricetulus migratorius* (Pallas, 1773) (Rodentia, Mammalia) population from the Toros Mountains (Turkey): with a special reference to the relation of *Cricetulus* and *Allocrietus* genera. *Folia Historico Naturalia Musei Matraensis* 18, 17–34.
- Hokr, Z., 1951. Methoda kvantitativního stanovení klimatuve čtvrtohorach podle ssavcích společenství. *Vestník Ústředního Ústavu Geologického* 18, 209–219.
- Huntley, B., Alfano, M.J., Allen, J.R.M., Pollard, D., Tzedakis, P.C., Beaulieu, J.L., de Gruger, E., Watts, B., 2003. European vegetation during Marine Oxygen Isotope Stage-3. *Quaternary Research* 59, 195–212.
- Jeannot, M., Cartonnet, M., 2000. La microfaune de la Chênélaz (Hostias, Ain). L'environnement et son influence sur la biométrie dentaire chez *Arvicola terrestris* (Rodentia, Mammalia). *Revue de Paleobiologie* 19, 475–492.
- Kälin, D., 1999. Tribe cricetini. In: Rössner, G.E., y Heissig, K. (Eds.), *The Miocene Land Mammals of Europe*. Verlag Dr. Friedrich Pfeil, München, pp. 367–375.
- Kershaw, A.P., Whitlock, C., 2000. Palaeoecological records of the last glacial–interglacial cycle: patterns and causes of change. *Palaeogeography, Palaeoclimatology, Palaeoecology* 155, 1–5.
- Koby, F.E., Spahni, J.C., 1956. Découverte dans le Quaternaire espagnol d'un petit hamster: *Allocrietus bursae* Schaub. *Eclogae Geologicae Helvetiae* 49, 543–545.
- Köppen, W., 1931. *Grundriß der Klimakunde*. De Gruyter, Berlin.
- Kowalski, K., Nadachowski, A., 1982. Rodentia. In: Kozłowski, J.K. (Ed.), *Excavation in the Bacho Kiro Cave (Bulgaria). Final report*. Państwowe Wydawnictwo Naukowe, Warszawa, pp. 45–51.
- Leroux, M., 1993. The Mobile Polar High: a new concept explaining present mechanisms of meridional air-mass and energy exchanges and global propagation of paleoclimatic changes. *Global and Planetary Change* 7, 69–93.
- Lloyd, A.H., Armbruster, W.S., Edwards, M.E., 1994. Ecology of a steppe-tundra gradient in interior Alaska. *Journal of Vegetation Science* 5, 897–912.
- Lundqvist, J., Saarnisto, M., 1995. Summary of project IGPC-253. *Quaternary International* 28, 9–18.
- Meteorological Office, 1972. *Tables of Temperature, Relative Humidity, Precipitation and Sunshine for the World: Part III. Europe and the Azores*. Her Majesty's Stationery Office, London.
- Meyer, H.-H., Kottmeier, C., 1989. Die atmosphärische Zirkulation in Europa im Hochglazial der Weichsel-Eiszeit-abgeleitet von Paläowind-Indikatoren und modellsimulationen. *Eiszeitalter und Gegenwart* 39, 10–18.
- Montuire, S., Michaux, J., Legendre, S., Aguilar, J.-P., 1997. Rodents and climate: 1. A model for estimating past temperatures using arvicolid (Mammalia: Rodentia). *Palaeogeography, Palaeoclimatology, Palaeoecology* 128, 187–206.
- Nadachowski, A., 1984. Morphometric variability of dentition of the Late Pleistocene voles (Arvicolidae, Rodentia) from Bacho Kiro Cave (Bulgaria). *Acta Zoologica Cracoviensia* 27, 149–176.
- Nadachowski, A., 1991. Systematics, geographic variation, and evolution of snow voles (*Chionomys*) based on dental characters. *Acta Theriologica* 36, 1–45.
- Navarro, N., Lécuyer, C., Montuire, S., Langlois, C., Martineau, F., 2004. Oxygen isotope compositions of phosphate from arvicoline teeth and Quaternary climatic changes, Gigny, French Jura. *Quaternary Research* 62, 172–182.
- Neftel, A., Oeschger, H., Staffelbach, T., Stauffer, B., 1988. CO₂ record in the Byrd ice core 50,000–5,000 years B.P. *Nature* 331, 609–611.
- NGICP Members, 2004. High-resolution record of Northern hemisphere climate extending into the last interglacial period. *Nature* 431, 147–151.
- Nieto, M., Rodríguez, J., 2003. Inferencia paleoecológica en mamíferos cenozoicos: limitaciones metodológicas. *Coloquios de Paleontología, Volumen Extraordinario* 1, 459–474.
- Nord Andreasen, T., 1997. Taxonomic status of *Desmana* (Insectivora) and *Spermophilus* (Rodentia) specimens from Danish Late Weichselian deposits. *Acta Zoologica Cracoviensia* 40, 229–236.
- Overpeck, J.T., Webb, R.S., Webb III, T., 1992. Mapping eastern North American vegetation change of the past 18 ka: No-analogs and the future. *Geology* 20, 1071–1074.
- Popov, V.V., Gerasimov, S., Marinska, M., 1994. Multivariate palaeoecological analysis of a late Quaternary small mammal succession from North Bulgaria. *Historical Biology* 8, 261–274.
- Ponel, P., 1995. Rissian, Eemian and Würmian Coleoptera assemblages from La Grande Pile (Vosges, France). *Palaeogeography, Palaeoclimatology, Palaeoecology* 114, 1–41.
- Prentice, I.C., Webb III, T., 1998. BIOME 6000: reconstructing global mid-Holocene vegetation—Patterns from palaeoecological records. *Journal of Biogeography* 25, 997–1005.
- Prentice, I.C., Guiot, J., Harrison, S.P., 1992. Mediterranean vegetation, lake levels and palaeoclimate at the Last Glacial Maximum. *Nature* 360, 658–660.
- Prentice, I.C., Sykes, M.T., Lautenschlager, M., Harrison, S.P., Denissenko, O., Bartlein, P.J., 1993. Modelling global vegetation patterns and terrestrial carbon storage at the last glacial maximum. *Global Ecology and Biogeography Letters* 3, 67–76.

- Prentice, I.C., Jolly, D., BIOME 6000 participants, 2000. Mid-Holocene and glacial-maximum vegetation geography of the northern continents and Africa. *Journal of Biogeography* 27, 507–519.
- PRISM Project Members, 1995. Middle Pliocene Palaeoenvironments of the Northern Hemisphere. In: Vrba, E.S., Denton, G.H., Partridge, T.C., Burckle, L.H. (Eds.), *Paleoclimate and Evolution: with Emphasis on Human Origins*. Yale Univ. Press, New Haven, pp. 242–248.
- Ray, N., Adams, J.M., 2001. A GIS-based vegetation map of the world at the Last Glacial Maximum (25,000–15,000 BP). *Internet Archaeology* 11, 1–44.
- Rivas Martínez, S., 1994. Clasificación bioclimática de la Tierra. *Folia Botanica Matritensis* 13, 1–27.
- Rivas Martínez, S., Sánchez Mata, D., Costa, M., 1999. North American boreal and western temperate forest vegetation. Syntaxonomical synopsis of the potential natural plant communities of North America II. *Itinera Geobotánica* 12, 5–316.
- Schweizer, M., 2002. Grotte de la Chênelaz (Hostias, Ain, France): Les grands Mammifères de la couche 6b. *Revue de Paleobiologie* 21, 803–818.
- Spaulding, W.G., 1991. Pluvial climatic episodes in North America and North Africa: types and correlation with global climate. *Palaeogeography, Palaeoclimatology, Palaeoecology* 84, 217–227.
- Strahler, A.N., Strahler, A.H., 1987. *Modern Physical Geography*. John Wiley and Sons, New York.
- Svendsen, J.I., Alexanderson, H., Astakhov, V.I., Demidov, I., Dowdeswell, J.A., Funder, S., Gataullin, V., Henriksen, M., Hjort, C., Houmark-Nielsen, M., Hubberten, H.W., Ingolfsson, O., Jakobsson, M., Kjaer, K.H., Larsen, E., Lokrantz, H., Lunkka, J.P., Lysa, A., Mangerud, J., Matiouchkov, A., Murray, A., Møller, P., Niessen, F., Nikolskaya, O., Polyak, L., Saarnisto, M., Siegert, C., Siegert, M.J., Spielhagen, R.F., Stein, R., 2004. Late Quaternary ice sheet history of northern Eurasia. *Quaternary Science Reviews* 23, 1229–1271.
- van Andel, T.H., 2002. The climate and landscape of the middle part of the Weichselian glaciation in Europe: the Stage 3 Project. *Quaternary Research* 57, 2–8.
- van de Weerd, A., Daams, R., 1978. Quantitative composition of rodent faunas in the Spanish Neogene and paleoecological implications. *Proceedings of the Koninklijke Nederlandse Akademie van Wetenschappen Serie B* 81, 448–473.
- von Koenigswald, W., 1978. Die Säugetierfauna des Mittel-Würms aus der Kemathenhöhle im Altmühltal (Bayern). *Mitteilungen Bayerischen Staatssammlung für Paläontologie und historische Geologie* 18, 117–130.
- Walter, H., 1970. *Vegetationszonen und Klima*. Eugen Ulmer, Stuttgart.
- Willis, K.J., van Andel, T.H., 2004. Trees or no trees? The environments of central and eastern Europe during the Last Glaciation. *Quaternary Science Reviews* 23, 2369–2387.
- Willis, K.J., Rudner, E., Sümegi, P., 2000. The Full-Glacial forests of Central and Southeastern Europe. *Quaternary Research* 53, 203–213.
- Willis, K.J., Rudner, E., Sümegi, P., 2001. Reply to Carcaillet and Vernet. *Quaternary Research* 55, 388–389.
- Woillard, G., 1979. The last interglacial–glacial cycle at Grande Pile in Northeastern France. *Bulletin du Société Belge de Géologie* 88, 51–69.
- Woillard, G.M., Mook, W.G., 1982. Carbon-14 dates at Grande Pile: correlations of land and sea chronologies. *Science* 215, 159–161.
- Woodcock, D.W., Wells, P.V., 1990. Full-glacial summer temperatures in eastern North America as inferred from Wisconsinan vegetational zonation. *Palaeogeography, Palaeoclimatology, Palaeoecology* 79, 305–312.
- Yurtsev, B.A., 1982. Relics of the xerophyte vegetation of Beringia in northeastern Asia. In: Hopkins, D.M., Matthews Jr., J.V., Schweger, C.E., Young, S.B. (Eds.), *Paleoecology of Beringia*. Academic Press, New York, pp. 179–194.
- Zimov, S.A., Churyrin, V.I., Oreshko, A.P., Chapin III, F.S., Reynolds, J.F., Chapin, M.C., 1995. Steppe-tundra transition: a herbivore-driven biome shift at the end of the Pleistocene. *The American Naturalist* 146, 765–794.